Pulsar Properties

For additional information about pulsars, see the books *Pulsar Astronomy* by Andrew Lyne and Francis Graham-Smith and *Handbook of Pulsar Astronomy* by Duncan Lorimer and Michael Kramer.

Known radio pulsars appear to emit short pulses of radio radiation with pulse periods between 1.4 ms and 8.5 seconds. Even though the word ***pulsar*** is a combination of "pulse" and "star," pulsars are not pulsating stars. Their radio emission is actually continuous but beamed, so any one observer sees a pulse of radiation each time the beam sweeps across his line-of-sight. Since the pulse periods equal the rotation periods of spinning neutron stars, they are quite stable. Even though the radio emission mechanism is not well understood, radio observations of pulsars have yielded a number of important results because:

(1) Neutron stars are physics laboratories providing extreme conditions (deep gravitational potentials, densities exceeding nuclear densities, magnetic field strengths as high as $B \sim 10^{14}$ or even 10^{15} gauss) not available on Earth.

(2) Pulse periods can be measured with accuracies approaching 1 part in 10^{16}, permitting exquisitely sensitive measurements of small quantities such as the power of gravitational radiation emitted by a binary pulsar system or the gravitational perturbations from planetary-mass objects orbiting a pulsar.

The radical proposal that neutron stars exist was made with trepidation by Baade & Zwicky in 1934: "*With all reserve we advance the view that a supernova represents the transition of an ordinary star into a new form of star, the* ***neutron star****, which would be the end point of stellar evolution. Such a star may possess a very small radius and an extremely high density.*" Pulsars provided the first evidence that neutron stars really do exist. They tell us about the strong nuclear force and the nuclear equation of state in new ranges of pressure and density, test general relativity and alternative theories of gravitation in both shallow and relativisitically deep ($GM/(rc^2) \gg 0$) potentials, and led to the discovery of the first extrasolar planets.

Discovery and Basic Properties

Pulsars were discovered serendipidously in 1967 on chart-recorder records obtained during a low-frequency ($\nu = 81$ MHz) survey of extragalactic radio sources that scintillate in the interplanetary plasma, just as stars twinkle in the Earth's atmosphere. This important discovery remains a warning against overprocessing data before looking at them, ignoring unexpected signals, and failing to explore observational "parameter space" (here the relevant parameter being time). As radio instrumentation and data-taking computer programs become more sophisticated, signals are "cleaned up" before they reach the astronomer and optimal "matched filtering" tends to suppress the unexpected. Thus clipping circuits are used to remove the strong impulses that are usually caused by terrestrial interference, and integrators smooth out fluctuations shorter than the integration time. Pulsar signals "had been recorded but not recognized" several years earlier with the 250-foot Jodrell Bank telescope. Most pulses seen by radio astronomers are just artificial interference from radar, electric cattle fences, etc., and short pulses from sources at astronomical distances imply unexpectedly high brightness temperatures $T_{\rm b} \sim 10^{25}$–10^{30} K $\gg 10^{12}$ K, the upper limit for incoherent electron-synchrotron radiation set by inverse-Compton scattering. However, Cambridge University graduate student Jocelyn Bell noticed pulsars in her scintillation survey data because the pulses appeared earlier by about 4 minutes every solar day, so they appeared exactly once per sidereal day and thus came from outside the solar system.

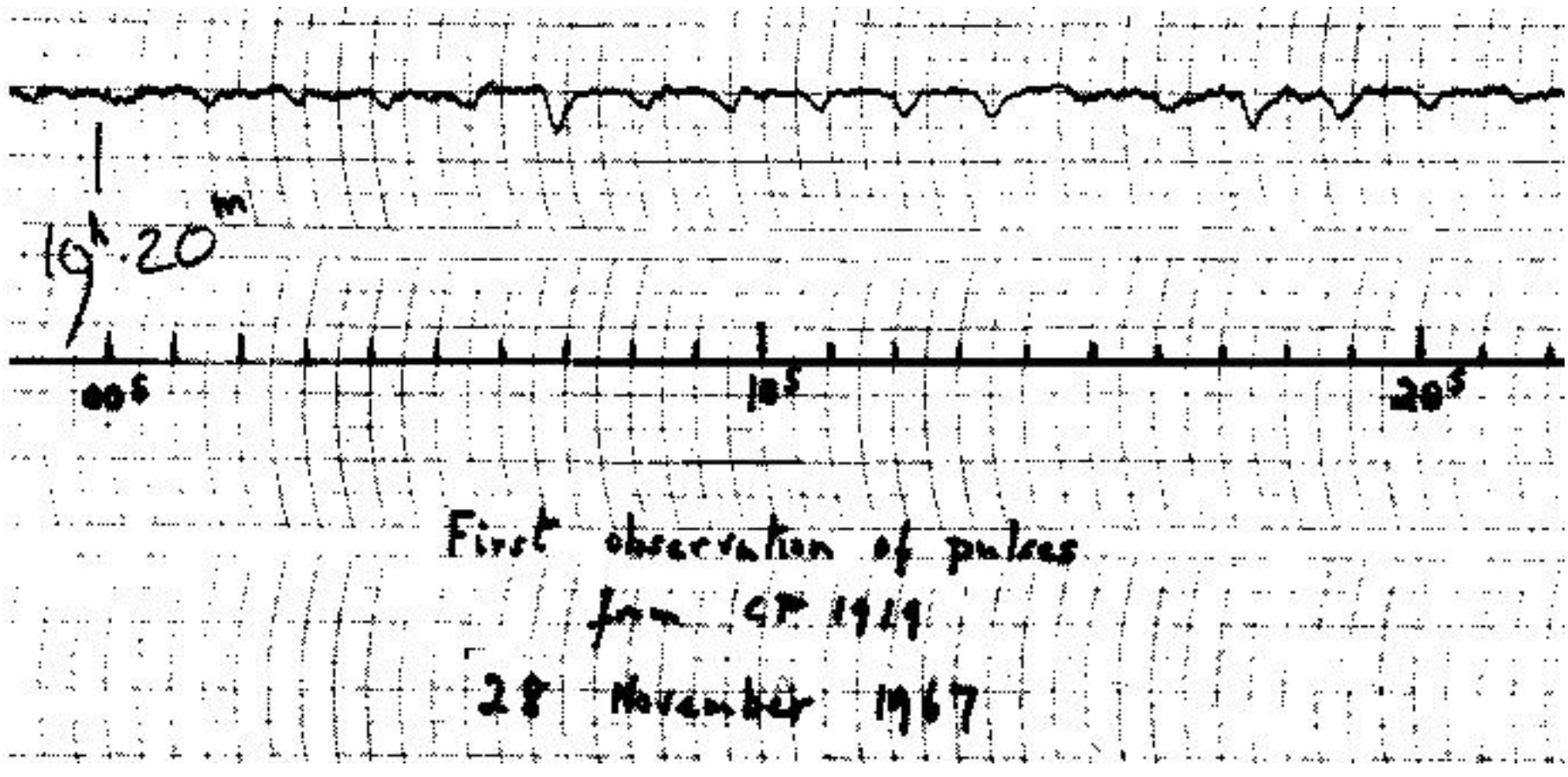

Figure 1. "High-speed" chart recording of the first known pulsar, CP1919. This confirmation observation showed that the "scruffy" signals observed previously were periodic.

The sources and emission mechanism were originally unknown, and even intelligent transmissions by LGM ("little green men") were seriously suggested as explanations for pulsars. Astronomers were used to slowly varying or pulsating emission from stars, but the natural period of a radially pulsating star depends on its mean density ρ and is typically days, not seconds. Likewise there is a lower limit to the rotation period P of a gravitationally bound star, set by the requirement that the centrifugal acceleration at its equator not exceed the gravitational acceleration. If a star of mass M and radius R rotates with angular velocity $\Omega = 2\pi/P$,

$$\Omega^2 R < \frac{GM}{R^2}$$

$$\frac{4\pi^2 R^3}{P^2} < GM$$

$$P^2 > \left(\frac{4\pi R^3}{3}\right)\frac{3\pi}{GM}$$

In terms of the mean density

$$\rho = M\left(\frac{4\pi R^3}{3}\right)^{-1},$$

$$P > \left(\frac{3\pi}{G\rho}\right)^{1/2}$$

or

$$\rho > \frac{3\pi}{GP^2} \qquad (6A1)$$

This is actually a very conservative lower limit to ρ because a rapidly spinning star becomes oblate, increasing the centrifugal acceleration and decreasing the gravitational acceleration at its equator.

Example: The first pulsar discovered (CP 1919+21, where the "CP" stands for *Cambridge pulsar*) has a period $P = 1.3$ s. What is its minimum mean density?

$$\rho > \frac{3\pi}{GP^2} = \frac{3\pi}{6.67 \times 10^{-8}\ \text{dyne cm}^2\ \text{gm}^{-2}(1.3\ \text{s})^2} \approx 10^8\ \text{g cm}^{-3}$$

This density limit is just consistent with the densities of white-dwarf stars. But soon the faster ($P = 0.033$ s) pulsar in the Crab Nebula was discovered, and its period implied a density too high for any stable white dwarf. The Crab nebula is the remnant of a known supernova recorded by ancient Chinese astronomers as a "guest star" in 1054 AD, so the discovery of this pulsar also confirmed the Baade & Zwicky suggestion that neutron stars are the compact remnants of supernovae. The fastest known pulsar has $P = 1.4 \times 10^{-3}$ s implying $\rho > 10^{14}$ g cm^{-3}, the density of nuclear matter. For a star of mass greater than the ***Chandrasekhar mass***

$$M_{\rm Ch} \approx \left(\frac{hc}{2\pi G}\right)^{3/2} \frac{1}{m_{\rm p}^2} \approx 1.4 M_\odot$$

(compact stars less massive than this are stable as white dwarfs), the maximum radius is

$$R < \left(\frac{3M}{4\pi\rho}\right)^{1/3}$$

In the case of the $P = 1.4 \times 10^{-3}$ pulsar with $\rho > 10^{14}$ g cm^{-3},

$$R < \left(\frac{3 \times 1.4 \times 2.0 \times 10^{33}\ \mathrm{g}}{4\pi \times 10^{14}\ \mathrm{g\ cm^{-3}}} \right)^{1/3} \approx 2 \times 10^{6}\ \mathrm{cm} \approx 20\ \mathrm{km}$$

The ***canonical neutron star*** has $M \approx 1.4 M_{\odot}$ and $R \approx 10$ km, depending on the equation-of-state of extremely dense matter composed of neutrons, quarks, etc. The extreme density and pressure turns most of the star into a neutron superfluid that is a superconductor up to temperatures $T \sim 10^{9}$ K. Any star of significantly higher mass ($M \sim 3 M_{\odot}$ in standard models) must collapse and become a black hole. The masses of several neutron stars have been measured with varying degrees of accuracy, and all turn out to be very close to $1.4 M_{\odot}$.

The Sun and many other stars are known to possess roughly dipolar magnetic fields. Stellar interiors are mostly ionized gas and hence good electrical conductors. Charged particles are constrained to move along magnetic field lines and, conversely, field lines are tied to the particle mass distribution. When the core of a star collapses from a size $\sim 10^{11}$ cm to $\sim 10^{6}$ cm, its magnetic flux $\Phi \equiv \int \vec{B} \cdot \vec{n}\, da$ is conserved and the initial magnetic field strength is multiplied by $\sim 10^{10}$, the factor by which the cross-sectional area a falls. An initial magnetic field strength of $B \sim 100$ G becomes $B \sim 10^{12}$ G after collapse, so young neutron stars should have very strong dipolar fields. The best models of the core-collapse process show that a dynamo effect may generate an even larger magnetic field. Such dynamos are thought to be able to produce the $10^{14} - 10^{15}$G fields in ***magnetars***, neutron stars having such strong magnetic fields that their radiation is powered by magnetic field decay. Conservation of angular momentum during collapse increases the rotation rate by about the same factor, 10^{10}, yielding initial periods in the millisecond range. Thus young neutron stars should drive rapidly rotating magnetic dipoles.

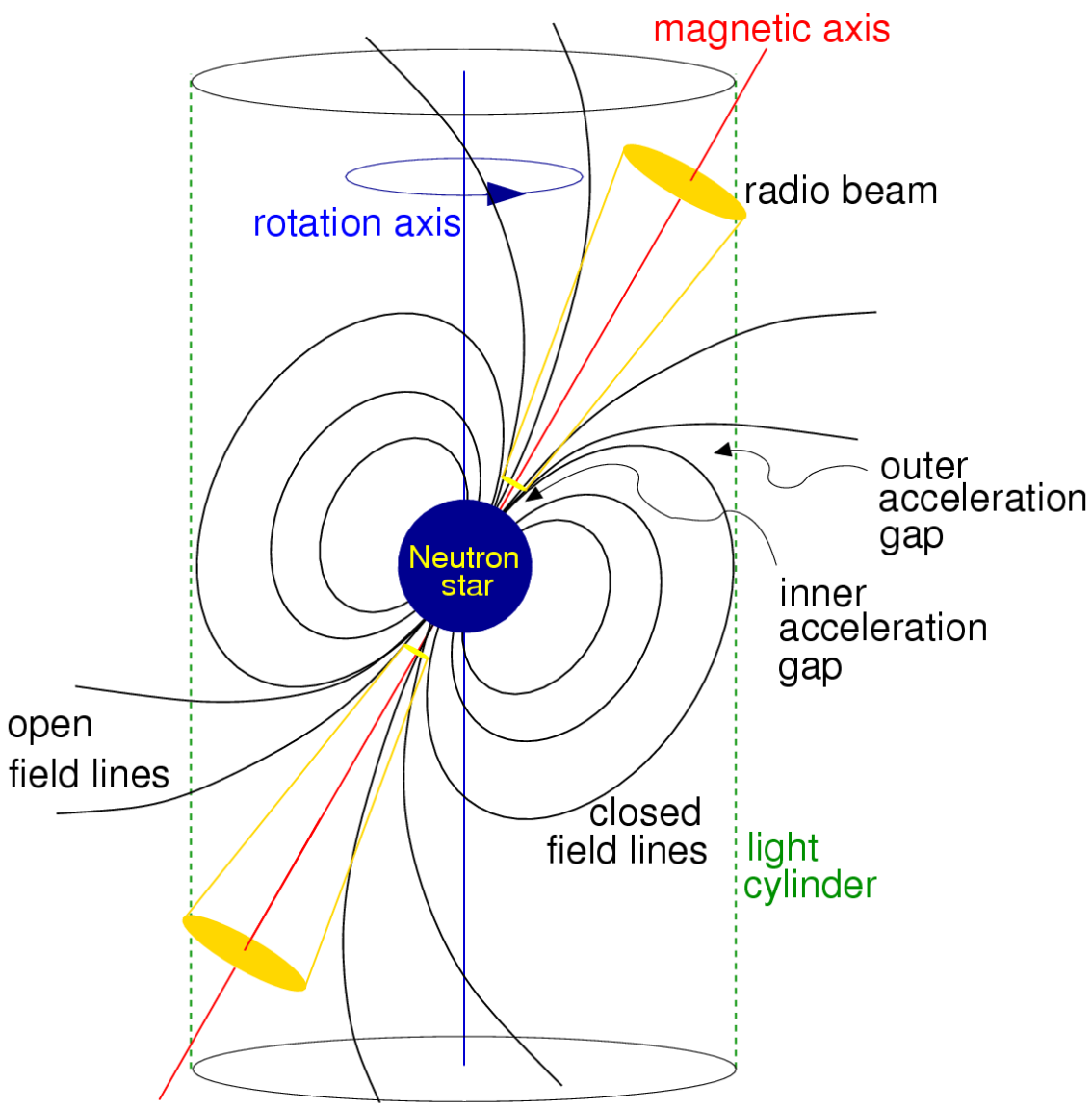

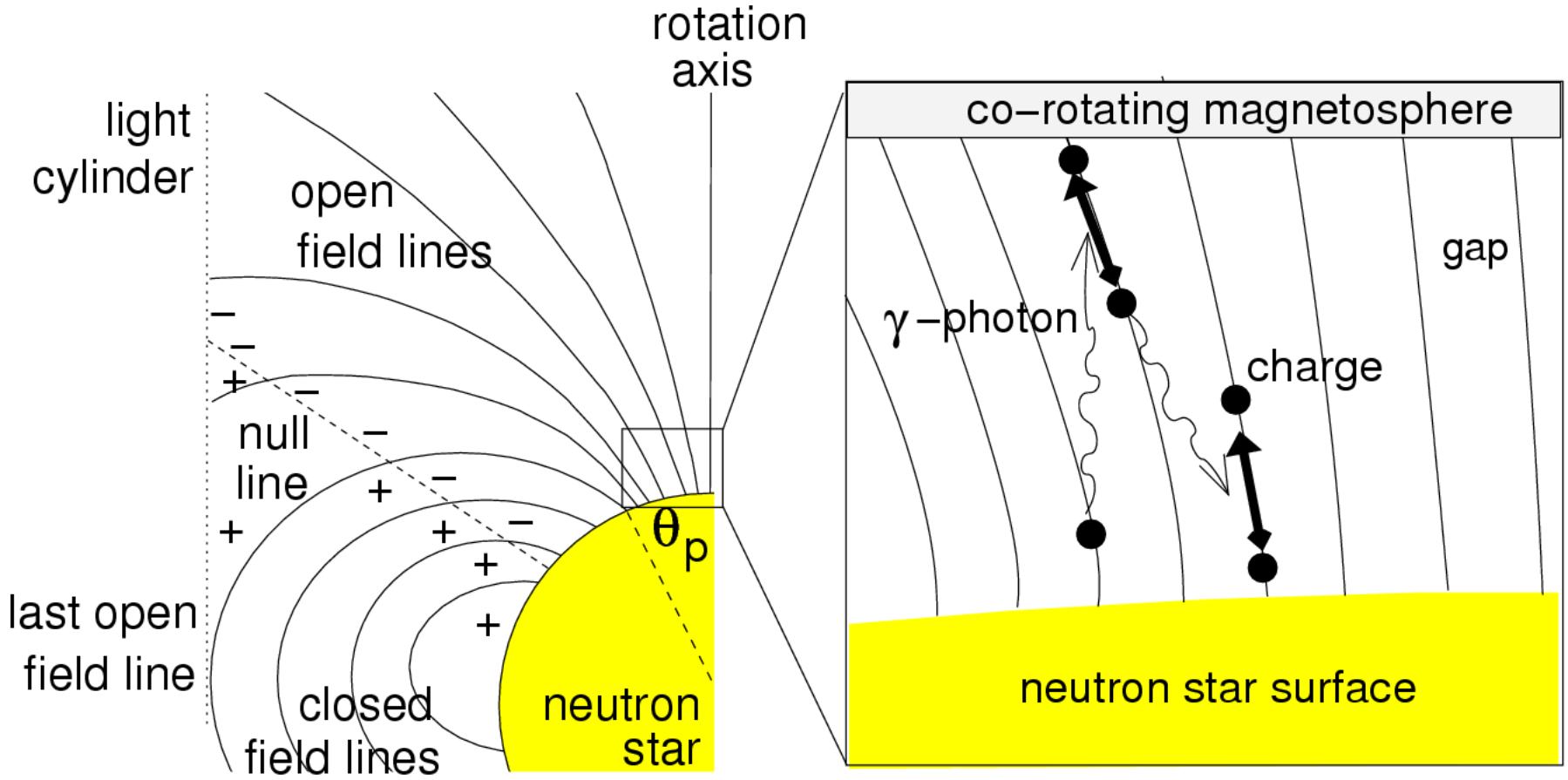

Figure 2: A Pulsar. (left or top): A diagram of the traditional magnetic dipole model of a pulsar. (right or bottom) Diagram of a simple dipole magnetic field near the polar caps. The inset figure shows a schematic of the electon-positron cascade which is required by many models of coherent pulsar radio emission (Both figures are from the Handbook of Pulsar Astronomy by Lorimer and Kramer).

Energetics

If the ***magnetic dipole*** is inclined by some angle $\alpha > 0$ from the rotation axis, it emits low-frequency electromagnetic radiation. Recall the Larmor formula for radiation from a rotating electric dipole:

$$P_{\rm rad} = \frac{2q^2\dot{v}^2}{3c^3} = \frac{2}{3}\frac{(q\ddot{r}\sin\alpha)^2}{c^3} = \frac{2}{3}\frac{(\ddot{p}_\perp)^2}{c^3} \ ,$$

where $p_\perp$ is the perpendicular component of the electric dipole moment. By analogy, the power of
the ***magnetic dipole radiation*** from an inclined magnetic dipole is

$$P_{\rm rad} = \frac{2}{3}\frac{(\ddot{m}_\perp)^2}{c^3} \qquad (6A2)$$

where $m_\perp$ is the perpendicular component of the magnetic dipole moment. For a uniformly magnetized sphere with radius R and surface magnetic field strength B, the magnetic dipole moment is (see Jackson's *Classical Electrodynamics*)

$$m = BR^3 \ .$$

If the inclined magnetic dipole rotates with angular velocity Ω,

$$m = m_0 \exp(-i\Omega t)$$

$$\dot{m} = -i\Omega m_0 \exp(-i\Omega t)$$

$$\ddot{m} = \Omega^2 m_0 \exp(-i\Omega t) = \Omega^2 m$$

so

$$P_{\rm rad} = \frac{2}{3}\frac{m_\perp^2\,\Omega^4}{c^3} = \frac{2m_\perp^2}{3c^3}\left(\frac{2\pi}{P}\right)^4 = \frac{2}{3c^3}(BR^3\sin\alpha)^2\left(\frac{2\pi}{P}\right)^4 ,$$

where P is the pulsar period. This electromagnetic radiation will appear at the *very* low frequency $\nu = P^{-1} < 1$ kHz, so low that it cannot be observed, or even propagate through the ionized ISM. The huge power radiated is responsible for pulsar slowdown as it extracts rotational kinetic energy from the neutron star. The absorbed radiation can also light up a surrounding nebula, the Crab nebula for example.

The rotational kinetic energy $E_{\rm rot}$ is related to the moment of inertia I by

$$E_{\rm rot} = \frac{1}{2}I\Omega^2 = \frac{2\pi^2 I}{P^2} .$$

Example: The moment of inertia of the "canonical" neutron star (uniform-density sphere with $M \approx 1.4M_\odot$ and $R \approx 10$ km) is

$$I = \frac{2}{5}MR^2 \approx \frac{2\cdot 1.4\cdot 2.0\times 10^{33}\ {\rm g}\cdot(10^6\ {\rm cm})^2}{5} \approx 10^{45}\ {\rm gm\ cm^2}$$

Therefore the rotational energy of the Crab pulsar ($P = 0.033$ s) is

$$E_{\rm rot} = \frac{2\pi^2 I}{P^2} \approx \frac{2\pi^2\cdot 10^{45}\ {\rm g\ cm^2}}{(0.033\ {\rm s})^2} \approx 1.8\times 10^{49}\ {\rm ergs}$$

Pulsars are observed to slow down gradually:

$$\dot{P} \equiv \frac{dP}{dt} > 0$$

Note that $\dot{P}$ is dimensionless (e.g., seconds per second). From the observed period P and period derivative $\dot{P}$ we can estimate the rate at which the rotational energy is decreasing.

$$\frac{dE_{\text{rot}}}{dt} = \frac{d}{dt}\left(\frac{1}{2} I \Omega^2\right) = I \Omega \dot{\Omega}$$

$$\Omega = \frac{2\pi}{P} \qquad \text{so} \qquad \dot{\Omega} = 2\pi(-P^{-2}\dot{P})$$

and

$$\frac{dE_{\text{rot}}}{dt} = I\Omega\dot{\Omega} = I\frac{2\pi}{P}\frac{2\pi(-\dot{P})}{P^2}$$

$$\frac{dE_{\text{rot}}}{dt} = \frac{-4\pi^2 I \dot{P}}{P^3} \qquad (6A3)$$

Example: The Crab pulsar has $P = 0.033$ s and $\dot{P} = 10^{-12.4}$. Its rotational energy is changing at the rate

$$\frac{dE_{\text{rot}}}{dt} = \frac{-4\pi^2 I \dot{P}}{P^3} = \frac{-4\pi^2 \cdot 10^{45}\ \text{g cm}^2 \cdot 10^{-12.4}\ \text{s s}^{-1}}{(0.033\ \text{s})^3} \approx -4 \times 10^{38}\ \text{erg s}^{-1}$$

Thus the low-frequency (30 Hz) magnetic dipole radiation from the Crab pulsar radiates a huge power $P_{\text{rad}} \approx -dE_{\text{rot}}/dt \approx 10^5 L_\odot$, comparable with the entire radio output of our Galaxy. It exceeds the Eddington limit, but that is not a problem because the energy *source* is not accretion. It greatly exceeds the average radio pulse luminosity of the Crab pulsar, $\sim 10^{30}$ erg s^{-1}. The long-wavelength magnetic dipole radiation energy is absorbed by and powers the Crab nebula (a "megawave oven").

Figure 3: Composite image of the Crab nebula. Blue indicates X-rays (from Chandra), green is optical (from the HST), and red is radio (from the VLA). *Image credit*

If we use $-dE_{\rm rot}/dt$ to estimate $P_{\rm rad}$, we can invert Larmor's formula for magnetic dipole radiation to find $B_\perp = B\sin\alpha$ and get a lower limit to the surface magnetic field strength $B > B\sin\alpha$, since we don't generally know the inclination angle α.

$$P_{\rm rad} = -\frac{dE_{\rm rot}}{dt}$$

$$\frac{2}{3c^3}(BR^3\sin\alpha)^2\left(\frac{4\pi^2}{P^2}\right)^2 = \frac{4\pi^2 I\dot{P}}{P^3}$$

$$B^2 = \frac{3c^3 IP\dot{P}}{2\cdot 4\pi^2 R^6\sin^2\alpha}$$

$$B > \left(\frac{3c^3 I}{8\pi^2 R^6}\right)^{1/2}(P\dot{P})^{1/2}$$

Evaluating the constants for the canonical pulsar in cgs units, we get

$$\left[\frac{3\cdot(3\times 10^{10}\ \mathrm{cm\ s^{-1}})^3\cdot 10^{45}\ \mathrm{g\ cm^2}}{8\pi^2(10^6\ \mathrm{cm})^6}\right]^{1/2} \approx 3.2\times 10^{19}$$

so the **minimum magnetic field** strength at the pulsar surface is

Example: What is the minimum magnetic field strength of the Crab pulsar

$$\left(\frac{B}{\text{Gauss}}\right) > 3.2 \times 10^{19} \left(P\dot{P}\right)^{1/2} \qquad \text{(6A4)}$$

($P = 0.033$ s, $\dot{P} = 10^{-12.4}$)?

$$\left(\frac{B}{\text{Gauss}}\right) > 3.2 \times 10^{19} \left(\frac{0.033 \text{ s} \cdot 10^{-12.4}}{\text{s}}\right) = 4 \times 10^{12}$$

This is an amazingly strong magnetic field. Its energy density is

$$U_B = \frac{B^2}{8\pi} > 5 \times 10^{23} \text{ erg cm}^{-3}$$

Just one cm^3 of this magnetic field contains over
5×10^{16} J $= 5 \times 10^{16}$ W s $= 1.6 \times 10^{9}$ W yr of energy, the annual output of a large nuclear power plant. A cubic meter contains more energy than has ever been generated by mankind.

If $(B \sin\alpha)$ doesn't change significantly with time, we can estimate a pulsar's

age τ from $P\dot{P}$ by assuming that the pulsar's initial period P_0 was much shorter than the current period. Starting with

$$B^2 = \frac{3c^3 I P \dot{P}}{8\pi^2 R^6 \sin^2\alpha}$$

we find that

$$P\dot{P} = \frac{8\pi^2 R^6 (B \sin\alpha)^2}{3c^3 I}$$

doesn't change with time. Rewriting the identity $P\dot{P} = P\dot{P}$ as $PdP = P\dot{P}\,dt$ and integrating over the pulsar's lifetime τ gives

$$\int_{P_0}^{P} PdP = \int_0^{\tau} (P\dot{P})\,dt = P\dot{P}\int_0^{\tau} dt$$

since $P\dot{P}$ is assumed to be constant over time.

$$\frac{P^2 - P_0^2}{2} = P\dot{P}\tau$$

If $P_0^2 \ll P^2$, the ***characteristic age*** of the pulsar is

$$\tau \equiv \frac{P}{2\dot{P}} \qquad (6A5)$$

Note that the characteristic age is not affected by uncertainties in the radius R, moment of inertia I, or $B \sin\alpha$; the only assumptions in its derivation are that $P_0 \ll P$ and that $P\dot{P}$ (i.e. B) is constant.

Example: What is the characteristic age of the Crab pulsar ($P = 0.033$ s,

$\dot{P} = 10^{-12.4}$)?

$$\tau = \frac{P}{2\dot{P}} = \frac{0.033 \text{ s}}{2 \cdot 10^{-12.4}} \approx 4.1 \times 10^{10} \text{ s} \approx \frac{4.1 \times 10^{10} \text{ s}}{10^{7.5} \text{ s yr}^{-1}} \approx 1300 \text{ yr}$$

Its actual age is about 950 years.

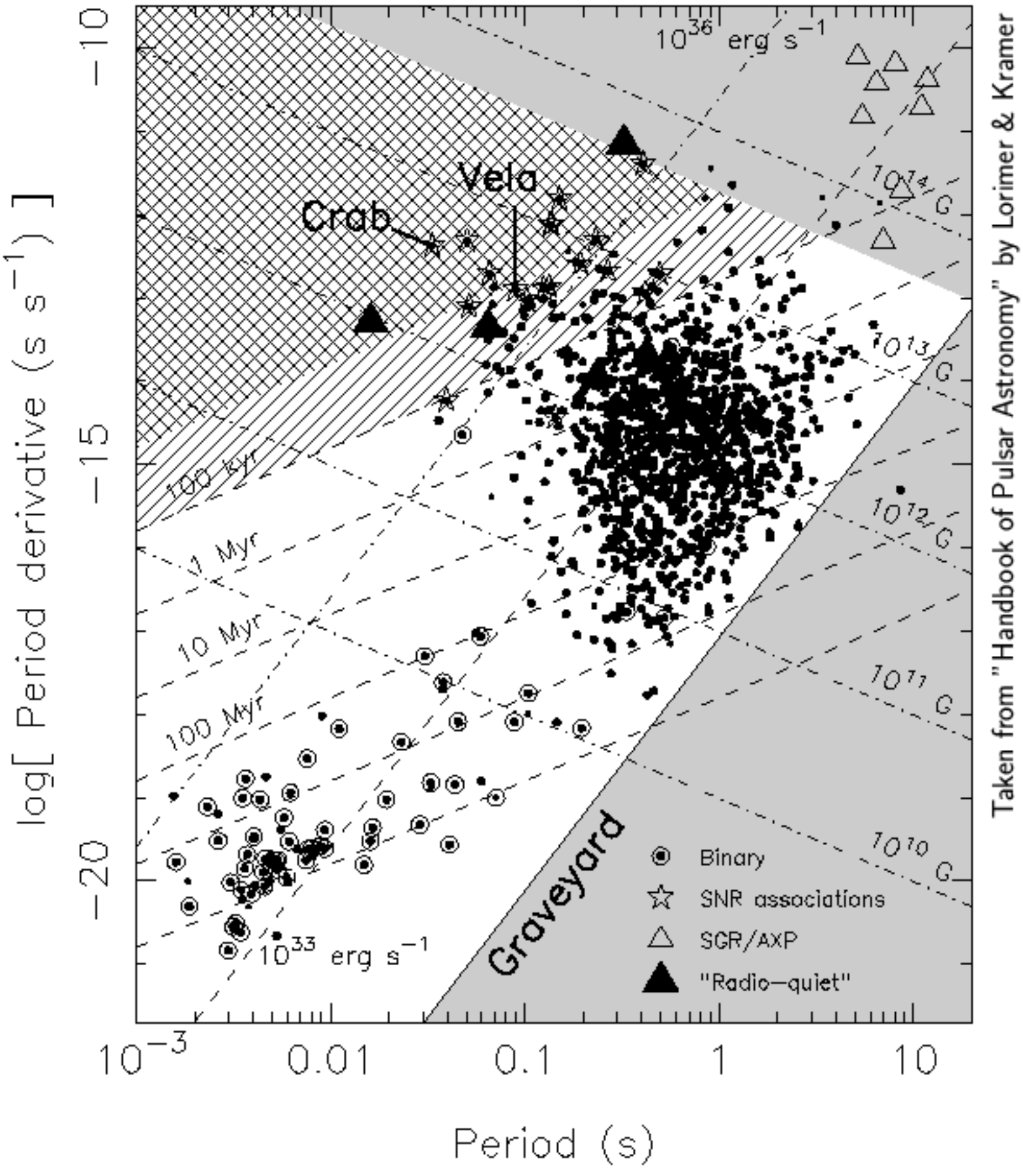

Figure 4: ***P-Pdot Diagram****. The $P\dot{P}$ diagram is useful for following the lives of pulsars, playing a role similar to the Hertzsprung-Russell diagram for ordinary stars. It encodes a tremendous amount of information about*

the pulsar population and its properties, as determined and estimated from

two of the primary observables, P and $\dot{P}$. Using those parameters, one can estimate the pulsar age, magnetic field strength B, and spin-down power

$\dot{E}$. (From the Handbook of Pulsar Astronomy, by Lorimer and Kramer)

The Lives of Pulsars

Pulsars are born in supernovae and appear in the upper left corner of the

$P\dot{P}$ diagram. If B is conserved and they age as described above, they gradually move to the right and down, along lines of constant B and crossing lines of constant characteristic age. Pulsars with characteristic ages $< 10^5$ yr are often found in or near recognizable supernova remnants. Older pulsars are not, either because their SNRs have faded to invisibility or because the supernova explosions expelled the pulsars with enough speed that they have since escaped from their parent SNRs. The bulk of the pulsar population is older than 10^5 yr but much younger than the Galaxy ($\sim 10^{10}$ yr). The observed distribution of pulsars in the $P\dot{P}$ diagram indicates that something changes as pulsars age. One controversial possibility is that the magnetic fields of old pulsars must decay on time scales $\sim 10^7$ yr, causing

old pulsars to move almost straight down in the $P\dot{P}$ diagram until they fall below into the graveyard below the ***death line*** and cease radiating radio pulses.

Almost all short-period pulsars below the ***spin-up line*** near

$\log[\dot{P}/P(\text{sec})] \approx -16$ are in binary systems, as evidenced by periodic (i.e. orbital) variations in their observed pulse periods. These ***recycled pulsars*** have been spun up by accreting mass and angular momentum from their companions, to the point that they emit radio pulses despite their relatively low magnetic field strengths $B \sim 10^8$ G (the accretion causes a substantial reduction in the magnetic field strength). The magnetic fields of neutron stars funnel ionized accreting material onto the magnetic polar caps, which become so hot that they emit X-rays. As the neutron stars rotate, the polar caps appear and disappear from view, causing periodic fluctuations in X-ray flux; many are detectable as X-ray pulsars.

Millisecond pulsars (MSPs) with low-mass ($M \sim 0.1 - 1 M_{\odot}$) white-dwarf companions typically have orbits with small eccentricities. Pulsars with extremely eccentric orbits usually have neutron-star companions, indicating that these companions also exploded as supernovae and nearly disrupted the binary system. Stellar interactions in globular clusters cause a much higher fraction of recycled pulsars per unit mass than in the Galactic disk. These interactions can result in very strange systems such as pulsar–main-sequence-star binaries and MSPs in highly eccentric orbits. In both cases, the original low-mass companion star that recycled the pulsar was ejected in an interaction and replaced by another star. (The ***eccentricity*** e of an elliptical orbit is defined as the ratio of the separation of the foci to the length of the major axis. It ranges between $e = 0$ for a circular orbit and $e = 1$ for a parabolic orbit.)

A few millisecond pulsars are isolated. They were probably recycled via the standard scenario in binary systems, but the energetic millisecond pulsars eventually ablated their companions away.

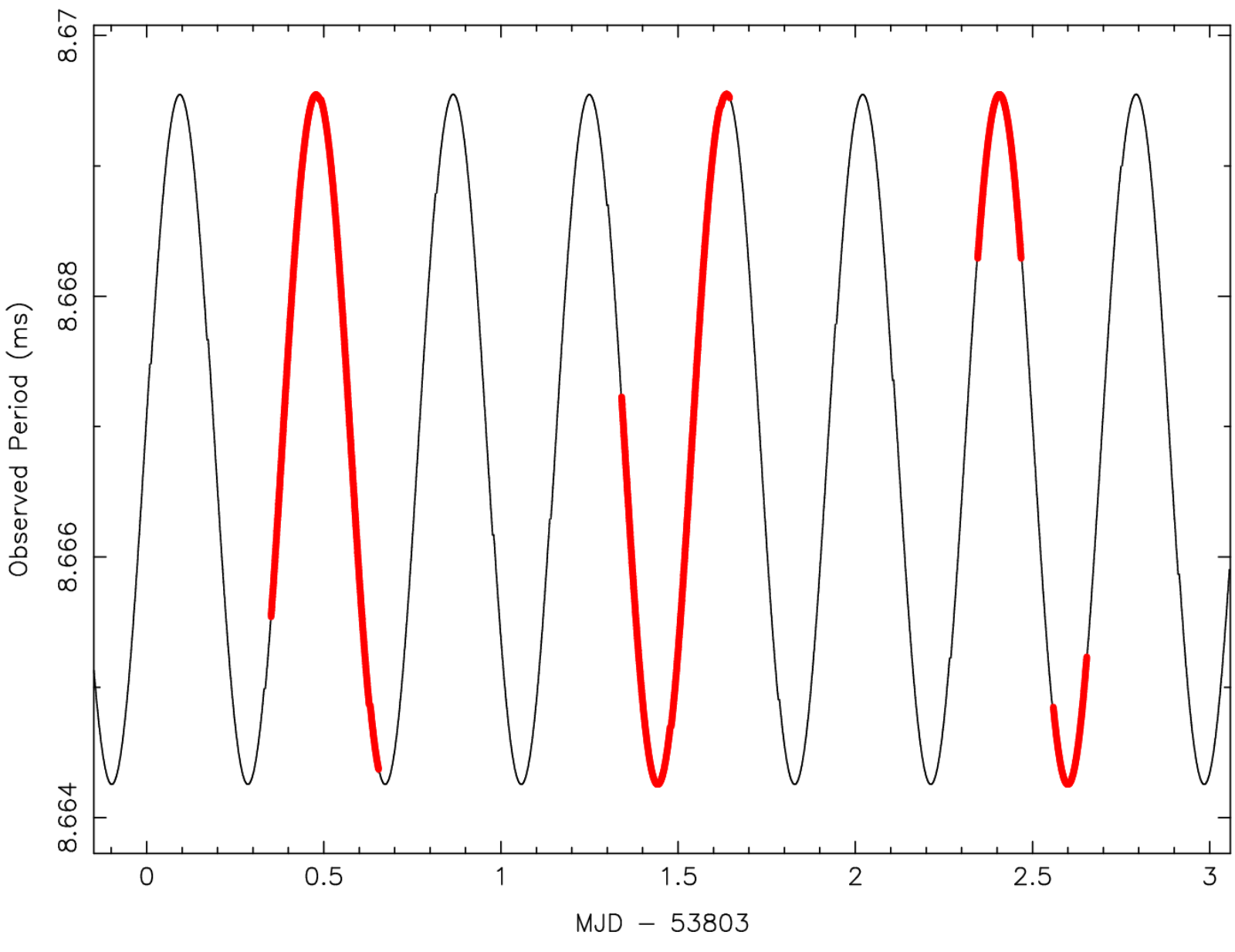

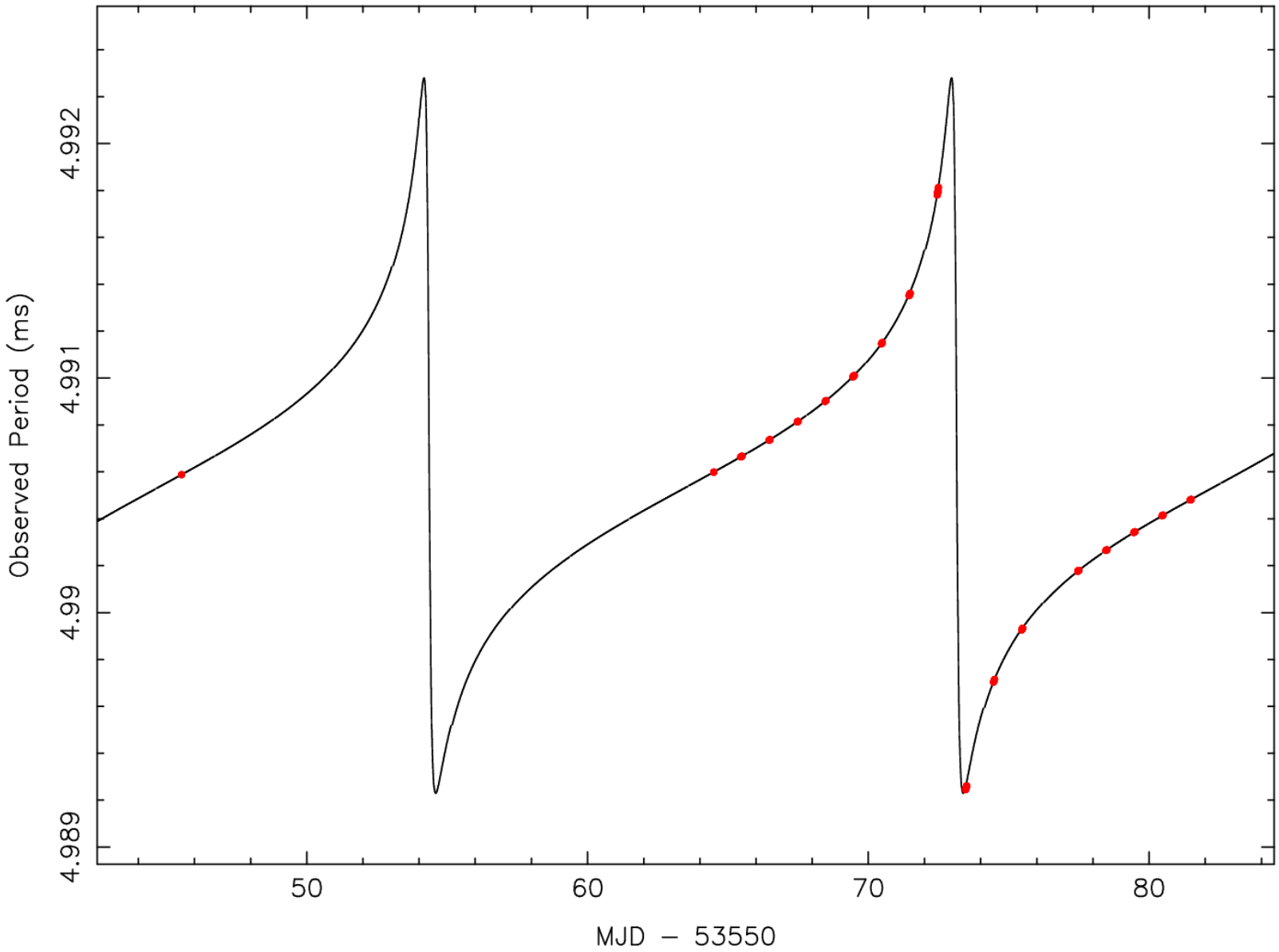

Figure 5: Examples of Doppler variations observed in binary systems containing pulsars. (left or top) The Doppler variations of the globular cluster MSP J1748−2446N in Terzan 5. This pulsar is in a nearly circular orbit (eccentricity $e = 4.6 \times 10^{-5}$) with a companion of minimum mass 0.47 $M_\odot$. The difference between the semi-major and semi-minor axes for this orbit is only 51±4 cm! The thick red lines show the periods as measured during GBT observations. (right or bottom) Similar Doppler variations from the highly eccentric binary MSP J0514−4002A in the globular cluster NGC 1851. This pulsar has one of the most eccentric orbits known ($e = 0.888$) and a massive white dwarf or neutron-star companion.

Emission Mechanisms

The radio pulses originate in the pulsar magnetosphere. Because the neutron star is a spinning magnetic dipole, it acts as a ***unipolar generator***. The total Lorentz force acting on a charged particle is

$$\vec{F} = q\left(\vec{E} + \frac{\vec{v} \times \vec{B}}{c}\right) .$$

Charges in the magnetic equatorial region redistribute themselves by moving along closed field

lines until they build up an electrostatic field large enough to cancel the magnetic force and give

$|\vec{F}| = 0$. The voltage induced is about 10^{16} V in MKS units. However, the co-rotating field lines emerging from the polar caps cross the ***light cylinder*** (the cylinder centered on the pulsar and aligned with the rotation axis at whose radius the co-rotating speed equals the speed of light) and these field lines cannot close. Electrons in the polar cap are magnetically accelerated to very high energies along the open but curved field lines, where the acceleration resulting from the curvature causes them to emit ***curvature radiation*** that is strongly polarized in the plane of curvature. As the radio beam sweeps across the line-of-sight, the plane of polarization is observed to rotate by up to 180 degrees, a purely geometrical effect. High-energy photons produced by curvature radiation interact with the magnetic field and lower-energy photons to produce electron-positron pairs that radiate more high-energy photons. The final results of this cascade process are bunches of charged particles that emit at radio wavelengths. The death line

in the $P\dot{P}$ diagram corresponds to neutron stars with sufficiently low B and high P that the curvature radiation near the polar surface is no longer capable of generating particle cascades. The extremely high brightness temperatures are explained by **coherent radiation**. The electrons do not radiate as independent charges e; instead bunches of N electrons in volumes whose dimensions are less than a wavelength emit in phase as charges Ne. Since Larmor's formula indicates that the power radiated by a chage q is proportional to q^2, the radiation intensity can be N^2 times brighter than incoherent radiation from the same total number N of electrons. Because the coherent volume is smaller at shorter wavelengths, most pulsars have extremely steep radio spectra. Typical (negative) pulsar spectral indices are $\alpha \sim 1.7$ ($S \propto \nu^{-1.7}$), although some can be much steeper ($\alpha > 3$) and a handful are almost flat ($\alpha < 0.5$).

Pulsars and the Interstellar Medium

(Note: the following closely follows the discussion in the *Handbook of Pulsar Astronomy* by Lorimer and Kramer)
With their sharp and short-duration pulse profiles and very high brightness temperatures, pulsars are unique probes of the interstellar medium (ISM). The electrons in the ISM make up a cold plasma having a refractive index

$$\mu = \left[1 - \left(\frac{\nu_{\rm p}}{\nu}\right)^2\right]^{1/2},$$

where ν is the frequency of the radio waves, $\nu_{\rm p}$ is the ***plasma frequency***

and n_e is the electron number density. For a typical ISM value $n_e \sim 0.03\ \mathrm{cm}^{-3}$, $\nu_p \sim 1.5$ kHz. If $\nu < \nu_p$ then μ is imaginary and radio waves cannot propagate through the plasma.

$$\nu_p = \left(\frac{e^2 n_e}{\pi m_e}\right)^{1/2} \approx 8.97\ \mathrm{kHz} \times \left(\frac{n_e}{\mathrm{cm}^{-3}}\right)^{1/2} \qquad (6A6)$$

For propagating radio waves, $\mu < 1$ and the ***group velocity*** $v_g = \mu c$ of pulses is less than the vacuum speed of light. For most radio observations $\nu_p \ll \nu$ so

A broadband pulse moves through a plasma more slowly at lower frequencies than at higher frequencies. If the distance to the source is d, the ***dispersion delay*** t at frequency ν is

$$v_g \approx c\left(1 - \frac{\nu_p^2}{2\nu^2}\right) \qquad (6A7)$$

$$t = \int_0^d v_g^{-1} dl - \frac{d}{c} = \frac{1}{c}\int_0^d \left(1 + \frac{\nu_p^2}{2\nu^2}\right) dl - \frac{d}{c}$$

$$= \frac{e^2}{2\pi m_e c}\frac{\int_0^d n_e dl}{\nu^2}.$$

In astronomically convenient units this becomes

where

$$\left(\frac{t}{\text{sec}}\right) \approx 4.149 \times 10^{3} \left(\frac{\text{DM}}{\text{pc cm}^{-3}}\right) \left(\frac{\nu}{\text{MHz}}\right)^{-2} \qquad \text{(6A8)}$$

in units of pc cm^{-3} is called the ***dispersion measure***.

$$\text{DM} \equiv \int_0^d n_e dl \qquad \text{(6A9)}$$

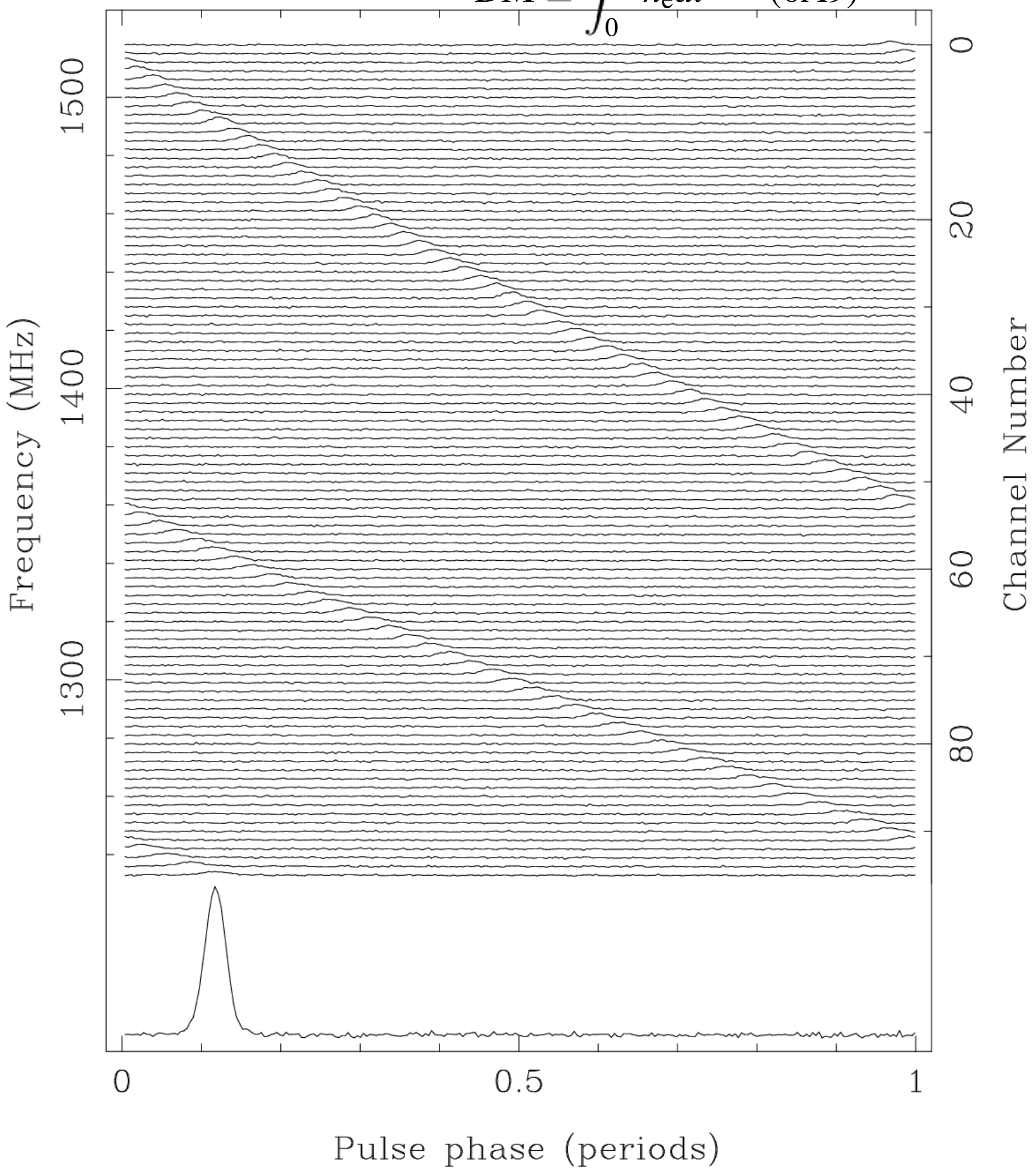

Figure 6: Pulsar dispersion. Uncorrected dispersive delays for a pulsar observation over a bandwidth of 288 MHz (96 channels of 3 MHz width each), centered at 1380 MHz. The delays wrap *since the data are folded (i.e. averaged) modulo the pulse period. (From the* Handbook of Pulsar Astronomy*, by Lorimer and Kramer)*

Measurements of the dispersion measure can provide distance estimates to pulsars. Crude estimates can be made for pulsars near the Galactic plane assuming that $n_e \sim 0.03$ cm^{-3}. However, several sophisticated models of the Galactic electron-density distribution now exist (e.g. NE2001; Cordes & Lazio 2002, astro-ph/0207156) that can provide much better ($\Delta d/d \sim 30\%$) distance estimates.

Since pulsar observations almost always cover a wide bandwidth, uncorrected differential delays across the band will cause ***dispersive smearing*** of the pulse profile. For pulsar searches, the DM is unknown and becomes a search parameter much like the pulsar spin frequency. This extra search dimension is one of the primary reasons that pulsar searches are computationally intensive.

Besides directly determining the integrated electron density along the line of site, observations of pulsars can be used to probe the ISM via absorption by spectral lines of HI or molecules (which can be used to estimate the pulsar distance as well), scintillation (allowing estimates of the pulsar transverse velocity), and pulse broadening.

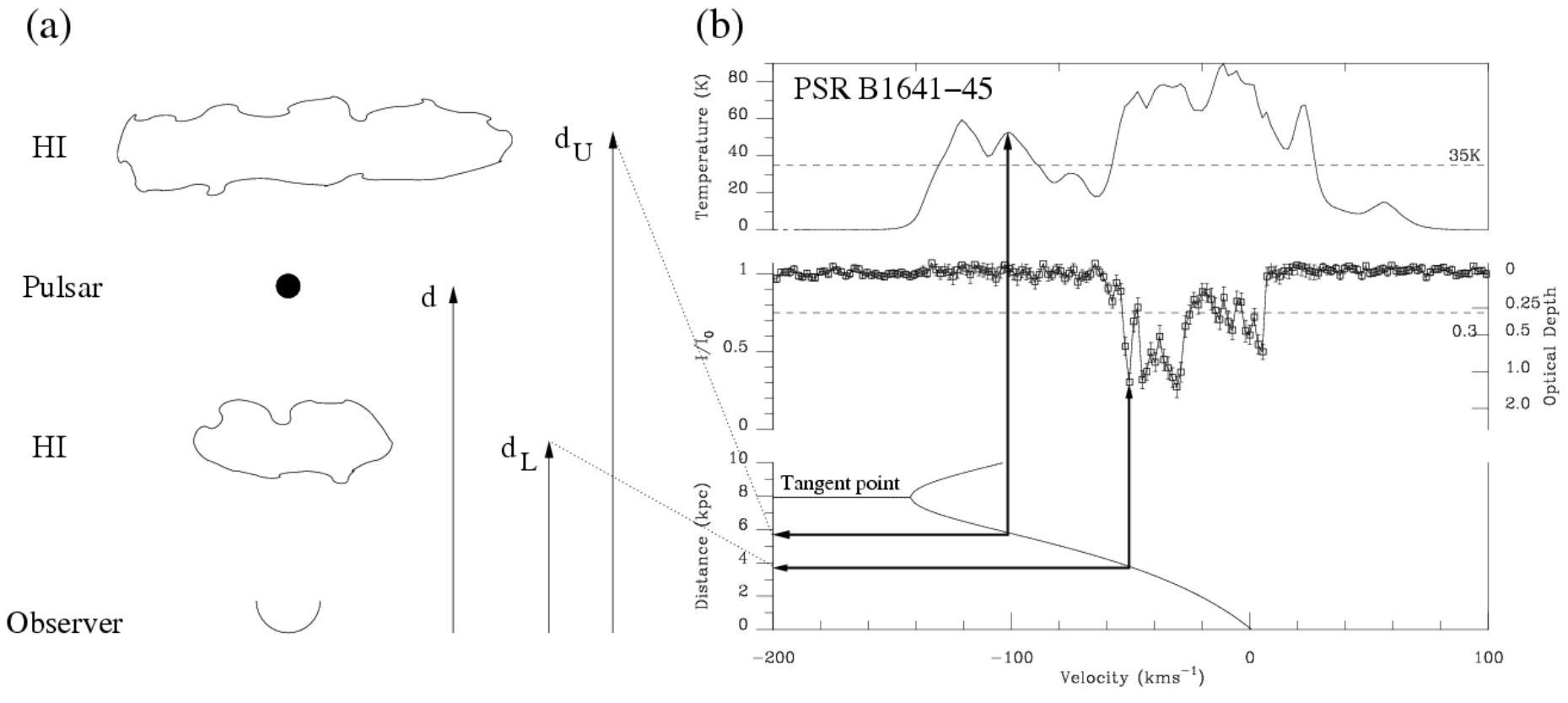

Figure 7: Pulsar HI Absorption Measurement. With a model for the Galactic rotation, such absorption measurements can provide pulsar distance

estimates or constraints. (From the Handbook of Pulsar Astronomy*, by Lorimer and Kramer)*

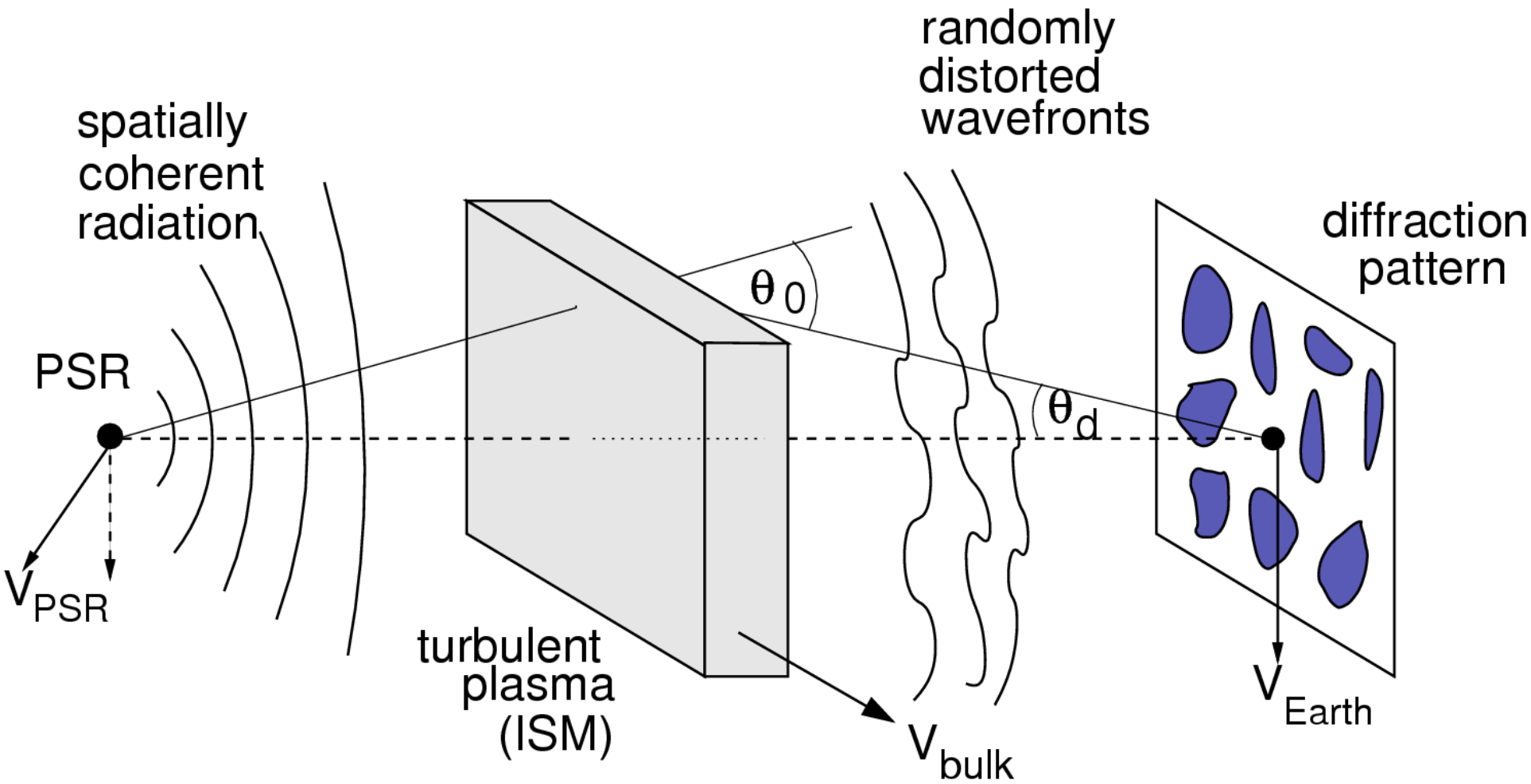

Figure 8: Thin Screen Diffraction/Scattering model. Inhomogeneities in the ISM cause small-angle deviations in the paths of the radio waves. These deviations result in time (and therefore phase) delays that can interfere to create a diffraction pattern, broaden the pulses in time, and make a larger image of the pulsar on the sky. (From the Handbook of Pulsar Astronomy*, by Lorimer and Kramer)*

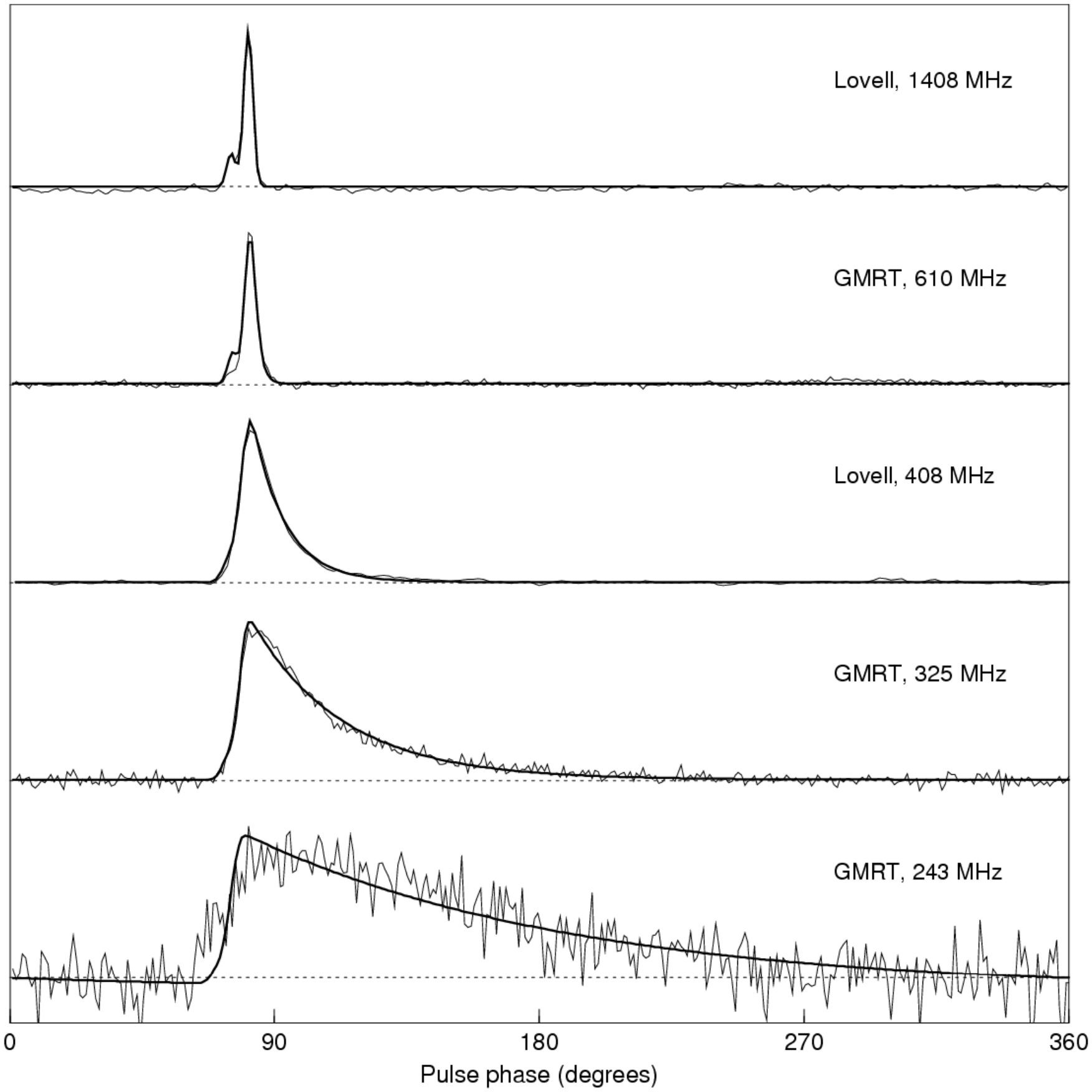

Figure 9: Pulse broadening caused by scattering. Scattering of the pulsed signal by ISM inhomogeneities results in delays that cause a scattering tail. This scatter-broadening can greatly decrease both the observational sensitivity and the timing precision for such pulsars. (From the Handbook of Pulsar Astronomy*, by Lorimer and Kramer)*

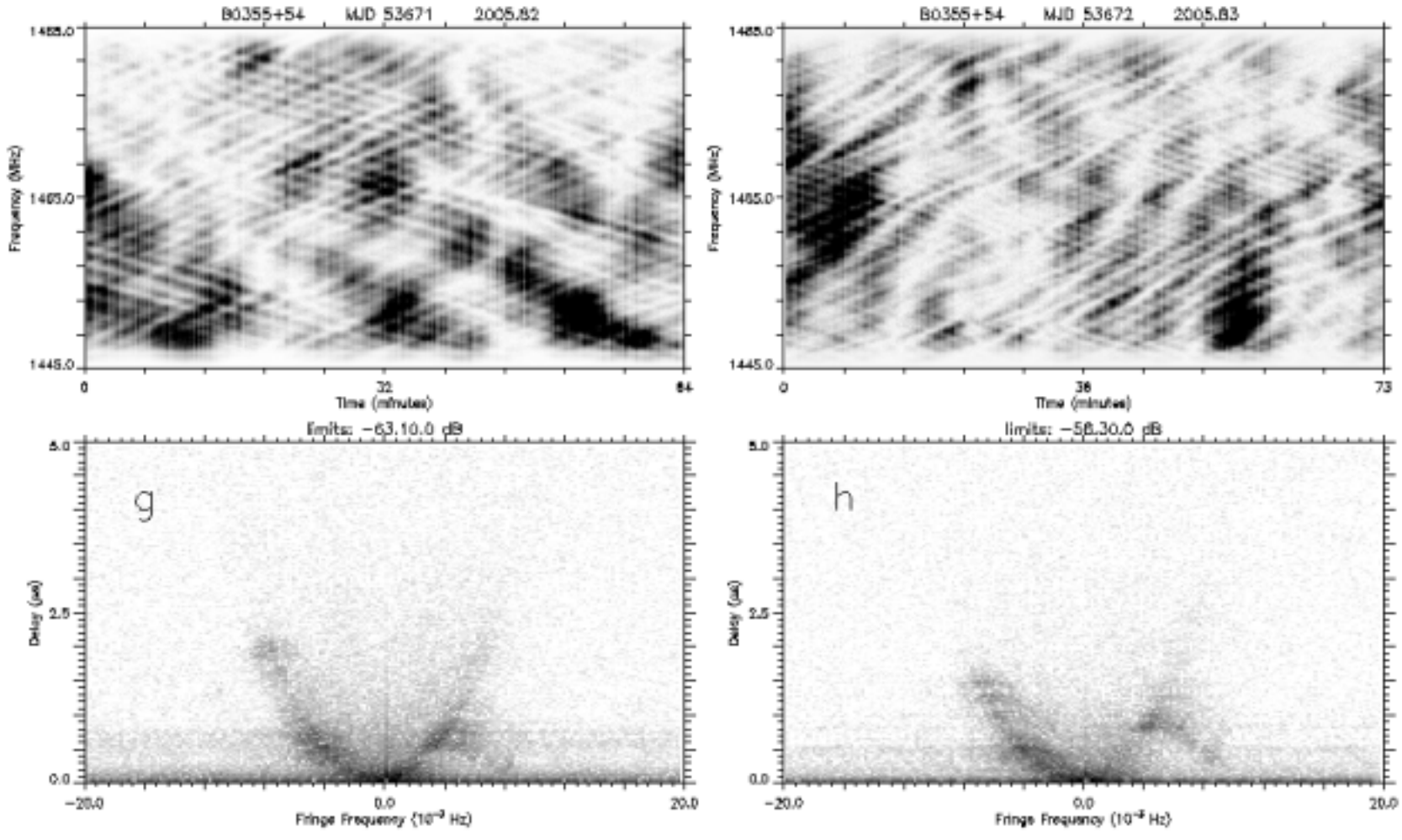

Figure 10: Diffractive Scintillation of a Pulsar. The top plots show dynamic spectra of the bright pulsar B0355+54 taken on two consecutive days with the GBT. The bottom plots show the so-called secondary spectra (the Fourier transforms of the dynamic spectra) and the so-called scintillation arcs (and moving arclets). (Figure provided by Dan Stinebring)